MULTIBODY DYNAMICS MODELING AND EXPERIMENTAL VALIDATION OF FUEL-INJECTION PUMP

Sundarraman P.[a], Baskaran R.[b], Sunilkumar V.[c] and Raghavendra K.[d]

Bosch Ltd., Adugodi, Bangalore – 560 030, India.
Email: [a]sundarraman.p@in.bosch.com, [b]baskaran.r@in.bosch.com
[c]sunilkumar.v@in.bosch.com, [d]k.raghavendra@in.bosch.com

Subir K. Saha

Dept. of Mech. Engg., IIT Delhi, New Delhi – 110 016, India.
Email: saha@mech.iitd.ac.in

Nilesh J. Vasa

Dept. of Engg. Design, IIT Madras, Chennai – 600 036, India.
Email: njvasa@iitm.ac.in

Fuel-Injection Pump (FIP) is used in diesel engines to generate pressure for fuel injection using a cam mechanism. With the advent of Fuel-Injection Equipment for high pressures, the design of FIP becomes critical not only with respect to the hydraulic system but also with respect to the multibody system. This paper proposes a methodology to model the multibody dynamic aspects of the FIP by applying a recursive MBD algorithm namely Decoupled Natural Orthogonal Complement (DeNOC) matrices. Such a model will be highly helpful in designing FIPs for high pressure application like common rail injection systems. The results based on the modeling are found to be in good agreement with other multibody dynamics software packages. Further, experimental studies are performed to estimate the driving torque and results are found to be in a good agreement with the model. This approach can be extended to a complex system comprising many similar moving bodies.

Keywords: Diesel fuel-injection pump, Cam-follower, multibody dynamic modeling.

1. INTRODUCTION

A Fuel-Injection Equipment (FIE) in a diesel engine comprises mainly a Fuel-Injection Pump (FIP) and fuel injector [1]. FIP pressurizes the fuel for injection, whereas the fuel injector injects it into the combustion chamber of engine.

1.1. The fuel-injection Pump

The cross section of a typical fuel-injection pump is shown in Figure 1(a). The plunger slides inside the barrel. The rotary drive from engine is converted into a reciprocating motion of the plunger by a higher-pair cam-mechanism in an FIP. A plunger return spring is used to ensure that the plunger returns back to the zero-lift position. The FIP works as follows [1]: As the plunger moves up, the pressure starts to build up when the inlet port, is closed by top-face of the plunger. As the plunger continues to move up, at some point, the pressure is relieved as the helix opens out the inlet port.

Research into Design — Supporting Sustainable Product Development. *Edited by* Amaresh Chakrabarti
 Published by Research Publishing
ISBN: 978-981-08-7721-7

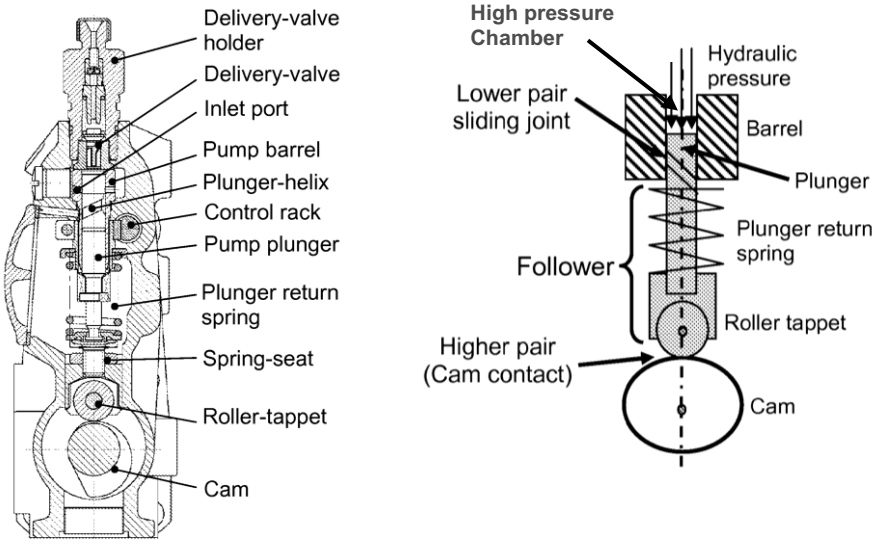

(a) Section of a Fuel-injection pump (b) Schematic mechanism diagram

Figure 1. The fuel-injection pump.

New generation diesel engines pose challenges with respect to meeting stringent emission norms and performance [2]. One way of achieving these low-emission requirements in diesel engines is by increasing the fuel pressure. In FIP, the pressure profile over the plunger lift depends mainly on the velocity curve of the cam as it determines the pressurization rate of fuel. The cam profile should also fulfill other requirements like sufficient lift to match the delivery volume and limiting the contact stress etc. Various sections like tangent, simple harmonic, polynomial etc. are used in designing cam profiles with which one can generate the discrete cam angle versus lift data spread in n number of values.

Design of an FIP for high pressure involves design and analysis of the mechanical and hydraulic system. With the advent of common rail systems, the pressure developed by these pumps have nearly doubled to the levels of 1600 bar today compared to the earlier conventional system. The drive train reaction forces and moments at various joints and the driving torque required to drive the pump etc. are all important when FIP has to be designed for high pressure applications. The model developed in this paper will be useful in estimating and hence optimizing the design parameters.

Application of FIP for high pressure offers some challenges in design like, (i) increased driving torque and power required by the pump from engine; (ii) increased loads on the moving bodies of the FIP; (iii) increased contact Hertz stress on cam-follower; (iv) increased reaction forces on the joints etc. The design of FIP for high pressure needs accurate estimation of these torque, forces and Hertz stress. This necessitates a multibody dynamics (MBD) model of FIP, which can estimate these forces accurately. Some research groups have attempted to study the FIP mechanism. Most of these work focuses on cam design [3] and experimental studies [4]. There are no reports on the modeling of FIP from the MBD point of view. An attempt is made to fill this gap by offering an approach to create an MBD model of a FIP. The MBD modeling of FIP involves two aspects: (i) Methodology to convert FIP into an MBD model (ii) Use of MBD approach to solve it. The focus of this paper is on the first aspect of MBD modeling with which one can apply any available methodology for the second aspect. From the forces calculated from this model the stresses in the components can be estimated and compared with material limits, to evolve at better cam profiles and designs.

The paper is organized as follows: In Section 2, the methodology of modeling the FIP is explained. In Section 3, the experimentation details are presented. Section 4 presents the results and discussions. Finally the conclusions are drawn in Section 5.

2. MODELING TECHNIQUE

2.1. The DeNOC methodology

To demonstrate the proposed approach, the Decoupled Natural Orthogonal Complement (DeNOC) matrices based approach for higher-pair cam based system proposed by Sundarraman and Saha [5] is used. This method is used as a tool to demonstrate the approach. However, any other relevant model which can develop the equations of motion of similar system can be used to build this model. This recursive approach uses the decoupled form of orthogonal complement matrix, which is derived from the system velocity constraints [6]. Such a recursive methodology helps in reducing the computation time when complex models including the engine and many FIPs have to be simulated. To validate the model, experimental studies were also performed on the FIP.

For modeling purpose, the simplified model of an FIP is shown in Figure 1(b). The cam-mechanism of FIP shown in Figure 1(b) will look similar to the one shown in Figure 2(a). The system has three bodies, a cam, a roller and a sliding follower. Various vectors are denoted in the figure and the parameters like pitch circle radius, base circle radius of cam and roller radius are denoted as, r_p, r_b and r_r respectively. The scalar, θ_1 denotes the cam rotation or joint variable at revolute joint 1 and scalar, θ_2 denotes the joint variable at revolute joint 2 at roller. The scalar, s is the linear displacement of the follower, i.e., the distance between O_2 and O_1 in Y_1-direction. As shown in Figure 2(a), $y(\theta_1)$ denotes the displacement equation of the cam with respect to its rotation angle, θ_1. The scalar, ϕ is the pressure angle, which can be defined using the displacement function and its derivative [7].

The modeling is performed in planar space, i. e. along the X_1-Y_1 plane of Figure 2, as most of the movement of FIP happens in planar space. Following are the assumptions made in the model, (i) Individual components are considered as rigid bodies; (ii) All the sliding components of the follower are considered as a single moving mass; (iii) Spring is considered to be a moving body with one-third of its mass; (iv) Spring stiffness is linear; (v) Pump rotational velocity is constant, and fluctuations due to engine strokes are neglected.

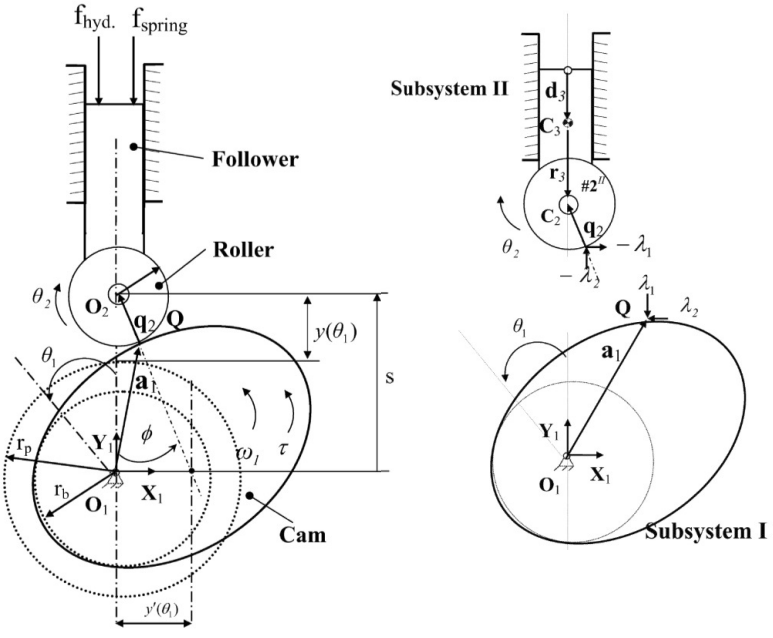

(a) Closed system (b) Open subsystems

Figure 2. Cam-mechanism with a roller-follower.

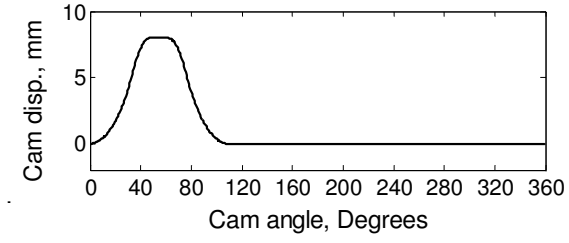

(a) Displacement in mm

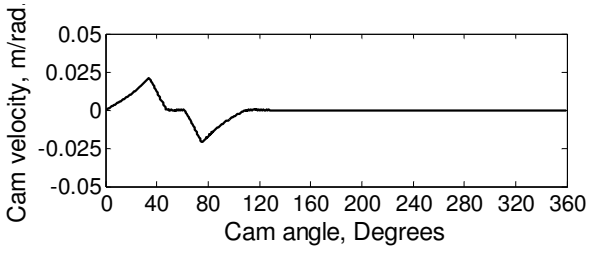

(b) Velocity in m/rad.

Figure 3. The spline interpolated displacement and velocity of cam-profile.

The model mainly focuses on inverse dynamics, where given a particular rotational velocity of pump various dynamic parameters are determined. Normally, the scalar angular speed of the cam shaft $\dot{\theta}_1$ as a function of time will be an input for such problems, as this is the main parameter to determine the FIP's performance. In general, a case of *constant* input rotational velocity at cam is considered in such applications.

Tsay *et al.* [8] have used splines to develop the displacement and velocity equations from the measured values of cam-profile. Using this methodology, the discrete displacement profile is interpolated to get a 3rd order piecewise continuous polynomial fit for angle versus lift. Its derivatives will give velocity and acceleration information. The cam rotation angle θ_1 can be determined from the input $\dot{\theta}_1$. Now, based on this angle, θ_1 the lift, $y(\theta_1)$, the velocity, $y'(\theta_1)$ and acceleration, $y''(\theta_1)$ with respect to cam angle, can be determined. The lift and velocity information with respect to the cam angle for an FIP based on the input of is presented in Figure 3, which comprises of forward stroke of 8 mm, dwell and return stroke. Based on the calculated velocity and acceleration profile of cam, the pressure angle and associated vectors can be determined [5]. To arrive at kinematic solution of the system, the loop-closure equations are used.

Dynamic input parameters like mass properties shall be obtained from the 3D models of the pump components. With the kinematic solution of the joint variables and dynamic data, any of the dynamic MBD models can be utilized in determining the time-dependent values of *driving torque* and other *constraint forces* at various joints.

However, the equations to be applied for the DeNOC based methodology for higher-pair system, explained in detail in [5], is given below briefly. The uncoupled (free-body) Newton-Euler (NE) equations of motion for *n*-bodies in a *serial system* with lower-pairs, such as a *revolute* or *prismatic* joint, are written as,

$$\mathbf{M}\dot{\mathbf{t}} + \mathbf{WMEt} = \mathbf{w} \tag{1}$$

In Equation 1, the $6n \times 6n$ matrices of *generalized mass*, **M**, *generalized angular velocity*, **W**, and *coupling*, **E**, are as defined in [6]. Also, the $6n-$dimensional vector of *generalised wrench*, **w** in right

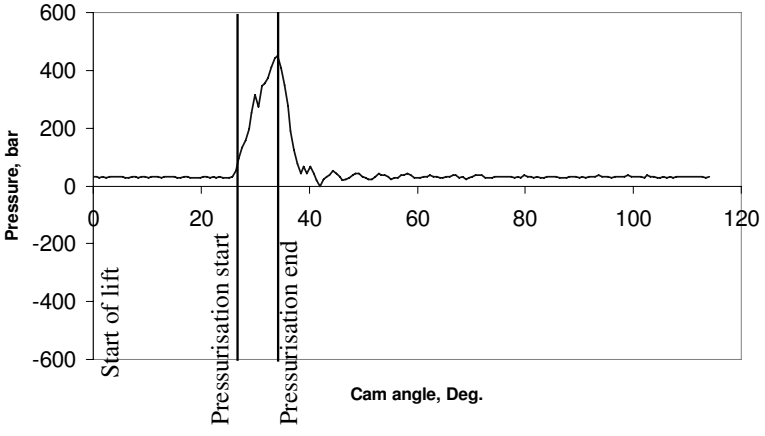

Figure 4. The spline interpolated displacement and velocity of cam-profile.

hand side of Equation 2 is given by,

$$\mathbf{w} = [\mathbf{w}_1^T \quad \mathbf{w}_1^T \quad \dots \quad \mathbf{w}_n^T]^T \tag{2}$$

which is the sum of generalized external moments and forces, $\mathbf{w}^e$ and *constraint moments and forces*, $\mathbf{w}^c$. The external forces applied in FIP model are the spring force and the hydraulic force in Y_1-direction. The spring stiffness coupled with the spring compression at zero-lift condition will give the spring preload. Dynamically, the lift at each instant gives the force due to spring. The hydraulic pressure on plunger is dependent on the pressure profile. Normally, the actual measured values or hydraulically simulated values of pressure versus cam angle are used to compute the hydraulic force acting on the plunger. These pressure values are spline interpolated with respect to cam rotation angle to have continuous hydraulic force being applied on the plunger during analysis. Figure 4 shows the measured fuel-pressure as a function of the cam rotation angle for an FIP. For about 20 degrees cam angle, till the plunger closes the inlet port, there is no pressurization taking place. After this, pressure starts to build and the pressurization continues till it reaches the peak value at around 30 degrees. As the fuel port is opened by the further movement of plunger, the pressure drops and reaches residual pressure. As it can be seen from Figures 3 and 4, the pressure curve follows the plunger velocity curve in the forward stroke.

The *generalized twist*, $\mathbf{t}$ for the serial body is written as,

$$\mathbf{t} = \mathbf{N}\dot{\theta} \quad \text{with } \mathbf{N} = \mathbf{N}_l\mathbf{N}_d \tag{3}$$

where, $\dot{\theta}$ is independent *joint-rate* vector of the serial system and $\mathbf{N}$ is the Natural Orthogonal Complement (NOC) matrix, which is the product of two matrices, $\mathbf{N}_l$ and $\mathbf{N}_d$, together called the Decoupled NOC matrices. The vector $\dot{\mathbf{t}}$ in Equation 1 is the *twist rate*.

The coupled NE equations of motion are then written using the NOC matrix as,

$$\mathbf{N}^T(\mathbf{M}\dot{\mathbf{t}} + \mathbf{WMEt}) = \mathbf{N}^T\mathbf{w}^\partial \tag{4}$$

where, $\mathbf{w}^e$ is the *generalized external wrench* as explained earlier. It has to be noted that, Equation 3 is not valid for a closed-loop system, as the vector, $\dot{\theta}$ (containing all active and passive *joint-rates*) is not independent. For applying any serial based approach, the vector needs to be independent. The FIP mechanism is a closed loop system, where each displacement variable (here θ_1, θ_2 and s) is related to each other using loop closure equations. Hence, to make it independent, the cam-mechanism of Figure 2(a) is cut along the contact point, Q as shown in Figure 2(b) to make it convenient to deal with higher-pair in equations. The two resulting subsystems are shown in Figure 2(b). After virtually cutting, the cam and follower become two independent serial subsystems referred as subsystems I and II, having one link and two links respectively with $\dot{\theta}_1$, $\dot{\theta}_2$ and $\dot{s}$ as joint variables. *Lagrange multipliers*

Table 1. Parameters for cam-follower mechanism of FIP.

Link no.	Base circle radius, r_b (m)	Mass, m_i (kg)	Moment of inertia about O_i, (kg-m^2)	Initial Position
1 (cam)	20×10^{-3}	0.25	5×10^{-5}	$\theta_1 = 0$ rad.
2 (follower)	—	0.075	—	$s = r_b$ m

Table 2. Dynamic parameters of FIP.

Cam and Roller	Radius, $r_r = 8 \times 10^{-3}$ m; Width, $B = 5 \times 10^{-3}$ m Coeff. of elasticity: $E_1 = E_2 = 210 \times 10^9$ N/m^2
Spring	Stiffness, $k = 20000$ N/m; Preload, $f_{s0} = 110$ N
Pump rotational speed, $\dot{\theta}_1$	500 rpm
Plunger diameter	8×10^{-3} m

are introduced at the cut-joint to substitute the removed *constraint moments and forces*. The vector of *Lagrange multipliers*, λ_2 and λ_2 denote the contact forces at the cut-joint, Q, along X_1 and Y_1-axes, respectively due to which a wrench will be acting on the subsystems. These subsystems are then solved using the methodology of serial systems as in [5].

The subsystem I has one constrained equation of motion with one unknown — driving torque, τ, which can be solved readily. The subsystem II has two equations with two unknowns — the two *Lagrange multipliers* as it has two bodies and two independent variables — $\dot{\theta}_2$ and s. These equations can also be solved for the Lagrange multipliers.

Having known these parameters and using the free-body equations given by Equation 1, the reaction forces and moments at each other joint can be determined. These are important for bearing design and stress evaluation.

2.2. The contact Hertz stress at cam-roller

For any cam-mechanism, contact Hertz stress acting on the cam and follower interface is critical for its life. The Hertz stress equation based on *cylindrical contact* theory [9] depends on the common normal force, f_{normal}, acting at the cam-follower interface, along the direction of the pressure angle ϕ and the instantaneous radius of cam, ρ_{cam}. The normal force, f_{normal} is the resultant of *Lagrange multipliers* which are determined from the DeNOC model.

2.3. The numerical example

Based on the kinematic and dynamic parameters of the FIP, described in Tables 1 and 2, a program is written in MATLAB to analyze FIP based on DeNOC methodology. The pressure profile of Figure 4 is used for hydraulic force input.

The results from the model are compared with commercial software and found to be closely matching.

3. EXPERIMENTAL STUDY

Figures 5(a) and 5(b) show the schematic diagram of the experimental setup and the pictorial view, respectively. An injector was connected to the pump using a high-pressure pipe. A strain-gauge based torque transducer (HBM model T22) is placed in between the cam-shaft and the drive motor. A pressure sensor (KISTLER type 4067A) was mounted on the high-pressure pipe at the pump end. The signal of end of pre-stroke (i.e. start of pressurization) was triggered using a proximity sensor in cam-shaft. The outputs of these sensors were connected to a data acquisition system. Under these conditions, the pressure and *driving torque* required by the pump was measured.

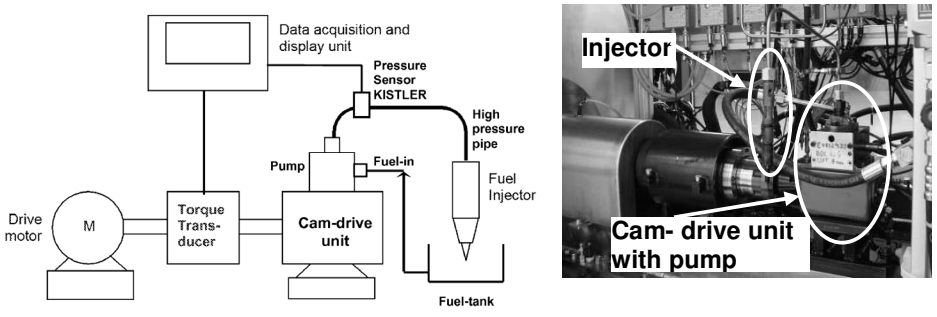

(a) Schematic layout (b) Pictorial view

Figure 5. Experimental setup.

4. RESULTS AND DISCUSSIONS

The measured pressure profile was already shown in Figure 4. As the delivery valve is present in between the high pressure chamber above the plunger (Figure 1(a)) and the high-pressure pipe, there will be some difference in pressure at the chamber and the high-pressure pipe. However, the measured pressures at the exit of the pump act as a representative of the pressures present in the chamber above the plunger. Figure 6 shows the temporal behavior of the measured and theoretically estimated *driving torque* for a part of the cycle where rise and fall takes place. In the forward direction, the measured value of *driving torque* is higher than the DeNOC model by about 10%. This difference may be due to various factors, such as (i) pressure in the chamber (above the plunger area) might be higher than what was being measured at the high-pressure pipe shown in Figure 5(a); (ii) loading effects like friction in cam-shaft bearings etc.; (iii) damping effects of lubricating oil filled in the cam-drive unit.

Also, from Figure 6, during the return stroke, the torque value of around -40 Nm was measured instead of about -5 Nm in the DeNOC model. This difference may be attributed to the high pressure that might be present in the pump chamber even during the initial stages of return stroke. Also, all the components were assumed to be rigid in the DeNOC based FIP model. However, in actual measurements, the stiffness of all the components in the drive line also would have played a role.

However, based on the experimentally measured values it is clear that the results of the *driving torque* from DeNOC model are in qualitative agreement with the measured values. Using this model, various other parameters like the Hertz stress, contact forces and the reaction forces at all the other

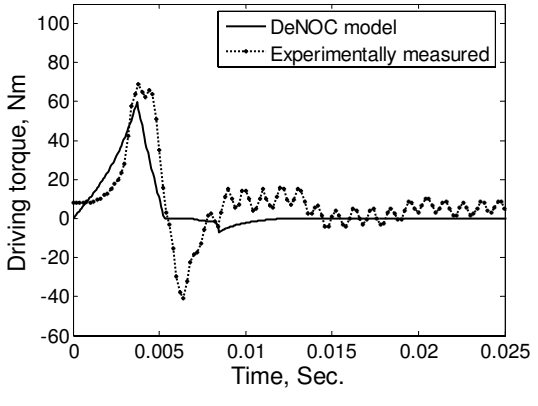

Figure 6. The driving torque at cam.

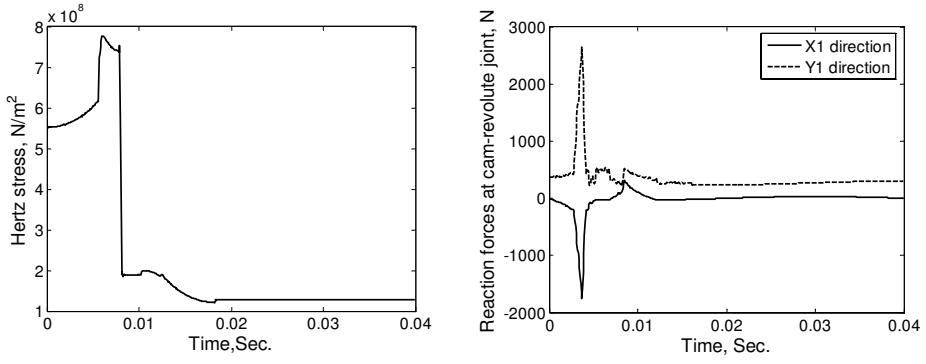

(a) Hertz stress at cam-roller interface (b) Reaction forces at cam revolute joint

Figure 7. Hertz stress and reaction forces.

joints can also be determined. For example, the results of Hertz stress at cam-roller interface and the reaction forces at the cam revolute joint are presented in Figures 7(a) and 7(b) respectively.

5. CONCLUSIONS

Modern diesel engines including the contemporary engines with common rail system use fuel injection pumps as a source of developing higher pressures. With these high pressure requirements, the design of these pumps becomes critical with respect to the moving parts involved in it. This paper offers a multibody modeling methodology for analyzing FIP cam-mechanism with a roller-follower, which can be used with any multibody modeling approach. The methodology is used to determine various design parameters, such as the driving torque and the reaction forces at various joints and results are in close agreement with that of commercial MBD software. Estimation of these parameters will be useful in designing and optimizing Fuel injection pumps for high pressure applications. Although experimentally measured driving torque values are about 10% higher than the theoretically predicted values, experimental results are in qualitative agreement with that of the theoretical model. The results can be used in better design, optimization study and failure analysis. The study has also pointed out that the driving torque and reaction forces will increase with increasing pressures. To reduce its impact, cam mechanism with offset follower axis shall be used.

REFERENCES

1. Robert Bosch GmbH, “Automotive Handbook”, 5th, Robert Bosch GmbH, Stuttgart, 2000.
2. Heywood, J. B., “Internal Combustion Engine Fundamentals”, McGraw Hill International Edition, 1988.
3. Kegl, B. and Muller, E., “An efficient cam design procedure for a prescribed diesel fuel injection rate profile using a Bezier curve”, International Congress & Exposition, Detroit, MI, USA, pp. 169 –176, 1998.
4. Tausenev, E. and Svistula, A., “The research into the disaxial cam mechanism for diesel fuel-injection pump”, Transport —2005, XX, pp. 225 –231, 2005 (Russian language).
5. Sundarraman, P. and Saha, S. K., “Multibody Dynamics Approach for the Analysis of Planar Mechanisms with Higher Pairs”, Multibody Dynamics 2009, ECCOMAS International Thematic Conference, Warsaw, Poland, 29 June 2 July, 2009.
6. Saha, S. K., “Dynamics of serial multibody systems using the Decoupled Natural Orthogonal Complement matrices”, Transactions of ASME, 66, pp. 986-996, December 1999.
7. Mallik, A. K., Ghosh, A., and Dittrich, G., “Kinematic Analysis and Synthesis of Mechanisms”, CRC Press, Inc., USA, 1994.
8. Tsay, D. M. Tsengl, K-S. and Chen, H-P., “A procedure for measuring planar cam profiles and their follower motions”, *Journal of Manufacturing Science and Engineering, ASME*, 128, pp. 697-704, 2006.
9. Norton, R. L., “Machine Design An Integrated Approach”, 3rd, Prentice Hall, New Jersey, 2006.